Remarks on Equivariant and Isovariant Maps between Representations

Ikumitsu NAGASAKI

STUDIA HUMANA et NATURALIA

No.47

京都府立医科大学医学部医学科

Kyoto Prefectural University of Medicine

2013年12月抜刷

Remarks on Equivariant and Isovariant Maps between Representations

Ikumitsu NAGASAKI [1)]

Abstract. In this note, we consider the existence problem of equivariant or isovariant maps between representation spheres. In particular, we give a necessary and sufficient condition for the existence of an equivariant map between unitary representation spheres of a cyclic group C_{pq}, where p, q are distinct primes.

1. The existence problem of C_{pq}-maps

The existence or non-existence problem of equivariant maps is a fundamental and important topic in equivariant topology, and many results are known up to the present. However, giving a necessary and sufficient condition for the existence of an equivariant map is not so easy in general. Recently, Marzantowicz, de Mattos and dos Santos [6] discuss a necessary and sufficient condition of the existence of an equivariant map for a torus and a p-torus. In this note, we deal with the case of C_{pq}-maps, where p, q are distinct primes.

First, we recall well-known results on the existence problem. Let G be a compact Lie group and V an (orthogonal) representation of G. We denote by SV the representation sphere of V, which is defined as the unit sphere of V. The following fact is proved by equivariant obstruction theory; for example, see [2].

Proposition 1.1. *Let V and W be (orthogonal) representations of G. If $\dim V^H \leq \dim W^H$ for every (closed) subgroup H of G, then there exists a G-map $f\colon SV \to SW$.*

The converse is not true in general, but in some special cases, the converse holds. Such kind of results are brought from Borsuk-Ulam type theorems. We state two Borsuk-Ulam type theorems; see [3], [4], [5], [11] for more details.

[1)] Department of Mathematics, Kyoto Prefectural University of Medicine, 13 Nishitakatsukasa-cho, Taishogun, Kita-ku, Kyoto 603-8334, Japan. e-mail: nagasaki@koto.kpu-m.ac.jp

2010 *Mathematics Subject Classification.* Primary 57S17; Secondary 55M20.

Proposition 1.2. *Assume that G acts freely on SV and SW. If there exists a G-map $f\colon SV \to SW$, then $\dim V \leq \dim W$ holds.*

Proposition 1.3. *Let G be a torus T^n or a p-torus C_p^n. Assume that SV and SW are G-fixed point free, i.e., $SV^G = SW^G = \emptyset$. If there exists a G-map $f\colon SV \to SW$, then $\dim V \leq \dim W$ holds.*

Marzantowicz, de Mattos and dos Santos [6] give a necessary and sufficient condition for the existence of an equivariant map in the case of G being a torus or a p-torus. In particular, the following result is deduced from their results.

Corollary 1.4. *Let G be a torus T^n or a p-torus C_p^n. Let SV and SW be G-fixed point free representation spheres. Then there exists a G-map $f\colon SV \to SW$ if and only if $\dim V^H \leq \dim W^H$ holds for every closed subgroups H of G.*

Proof. Note that G/H is a torus or a p-torus; in fact, if $G = T^n$, then G/H is connected and abelian. Hence G/H is a torus. If $G = C_p^n$, then G/H is an abelian group consisting of elements of order p or 1. Hence G/H is a p-torus. In each case, $f^H\colon SV^H \to SW^H$ is a G/H-map between G/H-fixed point free representation spheres. Hence Proposition 1.3 shows the necessary condition. The sufficient condition follows from Proposition 1.1. □

We now consider equivariant maps between representation spheres of a cyclic group C_{pq}, where p, q are distinct primes. Let $G = C_{pq}$ and c a generator of C_{pq}. The unitary irreducible representations U_k $(0 \leq k \leq pq-1)$ of C_{pq} are given by

$$cz = \xi^k z \quad \text{for} \quad z \in U_k = \mathbb{C},\ \xi = \exp\frac{2\pi\sqrt{-1}}{pq}.$$

Each orthogonal irreducible representation T_k is given as the following way: $T_0 = \mathbb{R}$ with the trivial action; if $0 < k < pq/2$, then $T_k = r_{\mathbb{R}}U_k$, where $r_{\mathbb{R}}$ denote realification of a unitary representation, and if $q = 2$ and p is an odd prime, then $T_p = \mathbb{R}_-$ with the antipodal action of C_2 and the trivial action of C_p.

Set $C_p = \langle c^q \rangle$ and $C_q = \langle c^p \rangle$. Let V and W be orthogonal representations with $V^G = W^G = 0$. If there exists a G-map $f\colon SV \to SW$, then $f^H\colon SV^H \to SW^H$ is a G/H-map for $H = C_p$ or C_q. Since G/H acts freely on SV^H and SW^H, it follows from Proposition 1.2 that $\dim V^H \leq \dim W^H$ for $H = C_p$, C_q. In the case of $\dim W^H = 0$ $(H = C_p$ or $C_q)$, it follows that $\dim V^H = 0$. Since $\mathrm{res}_H f$ is an H-map between H-free

representation spheres, we have $\dim V \leq \dim W$ by Proposition 1.2. Thus we obtain the following.

Proposition 1.5. *Let $G = C_{pq}$. Let V and W be representations with $V^G = W^G = 0$. If there exists a G-map $f: SV \to SW$, then the following hold.*

(1) $\dim V^{C_p} \leq \dim W^{C_p}$ *and* $\dim V^{C_q} \leq \dim W^{C_q}$.

(2) *If* $\dim W^{C_p} = 0$ *or* $\dim W^{C_q} = 0$, *then* $\dim V \leq \dim W$.

In the next section, we show that if V and W are unitary, then the converse holds. As a consequence, we obtain the following.

Theorem 1.6. *Let V and W be unitary representations with $V^G = W^G = 0$ for $G = C_{pq}$. There exists a G-map $f: SV \to SW$ if and only if the conditions* (1) *and* (2) *of Proposition* 1.5 *hold.*

2. Proof of Theorem 1.6

We have already shown that the conditions (1) and (2) are necessary. Next we show that (1) and (2) are sufficient for the existence of a G-map. The proof is divided into several cases.

We set $G = C_{pq}$ and denote by U_k the unitary irreducible representation of C_{pq} described in the previous section. The following is straightforward.

Lemma 2.1. *If $f_i: SV_i \to SW_i$, $i = 1, 2$, are G-maps, then the join of f_1 and f_2 induces a G-map $f_1 * f_2: S(V_1 \oplus V_2) \to S(W_1 \oplus W_2)$.*

The kernel $\operatorname{Ker} V$ of a representation V is defined by the kernel of the representation homomorphism of V: $\rho_V: G \to GL(V)$. It is easily seen that

$$\operatorname{Ker} U_k = \begin{cases} 1 & (k, pq) = 1 \\ C_p & (k, pq) = p \\ C_q & (k, pq) = q \\ C_{pq} & k = 0, \end{cases}$$

where (k, pq) denotes the greatest common divisor of k and pq.

Lemma 2.2. *If $\operatorname{Ker} U_k = \operatorname{Ker} U_l$, then there exists a G-map $f: SU_k \to SU_l$.*

Proof. If $\operatorname{Ker} U_k = \operatorname{Ker} U_l = C_{pq}$, then it is trivial. Assume that $\operatorname{Ker} U_k = \operatorname{Ker} U_l \neq C_{pq}$ Since $(k/(k, pq), pq) = 1$, one can take an integer s such that $sk/(k, pq) \equiv 1 \pmod{pq}$.

Then a map f defined by

$$f(z) = z^{sl/(k,pq)},\ z \in SU_k$$

is a G-map. □

For a representation V with $V^G = 0$, decompose V into irreducible representations as follows:

$$V = \bigoplus_{i=1}^{pq-1} a_i U_i\ (a_i \geq 0).$$

Let H be a subgroup of G. Setting $V(H) = \bigoplus_{i:\mathrm{Ker}\, U_i = H} a_i U_i$, we have a decomposition

$$V = V(1) \oplus V(C_p) \oplus V(C_q).$$

By Lemmas 2.1 and 2.2, we obtain the following.

Proposition 2.3. *There exist G-maps between $S(V(H))$ and $S(mU_{(|H|,pq)})$ bidirectionally, where $m = \frac{1}{2}\dim V(H)$.*

By this proposition, without loss of generality, we may assume that V and W have the following forms:

$$V = a_1 U_1 \oplus a_p U_p \oplus a_q U_q,$$
$$W = b_1 U_1 \oplus b_p U_p \oplus b_q U_q,$$

where a_i and b_i are non-negative integers. Note that $V^{C_p} = a_p U_p$, $V^{C_q} = a_q U_q$ and so on. It is easy to see that the conditions (1) and (2) are equivalent to statements:

(1) $a_p \leq b_p$ and $a_q \leq b_q$.

(2) If $b_p = 0$, then $a_1 + a_q \leq b_1 + b_q$ and if $b_q = 0$, then $a_1 + a_p \leq b_1 + b_p$.

First we recall the following result from [12].

Lemma 2.4. *Let $W = b_1 U_1 \oplus b_p U_p \oplus b_q U_q$, $b_p > 0$, $b_q > 0$. Then there exists a self G-map $h\colon SW \to SW$ such that* $\deg h = 0$.

Proof. Degrees of h^H, $H \leq G$, of a self G-map h on SW satisfy the Burnside ring relation described in [2]. In fact, it is seen that if there exists a G-map $h\colon SW \to SW$, then the following relations hold:

$$\begin{cases} \deg h \equiv \deg h^{C_p} \bmod p, \\ \deg h \equiv \deg h^{C_q} \bmod q, \\ \deg h^{C_p} \equiv 1 \bmod q, \\ \deg h^{C_q} \equiv 1 \bmod p. \end{cases}$$

Conversely, if integers d_1, d_p, d_q satisfy relations $d_1 \equiv d_p \bmod p$, $d_1 \equiv d_q \bmod q$, $d_p \equiv 1 \bmod q$ and $d_q \equiv 1 \bmod p$, then there exists a G-map $h\colon SW \to SW$ such that $\deg h = d_1$, $\deg h^{C_p} = d_p$, $\deg h^{C_q} = d_q$. We set $d_1 = 0$ and we can take d_p such that $d_p \equiv 0 \bmod p$, $d_p \equiv 1 \bmod q$ and d_q such that $d_q \equiv 1 \bmod p$, $d_q \equiv 0 \bmod q$, These integers satisfy the above relations. Therefore there exists a G-map $h\colon SW \to SW$ such that $\deg h = 0$. □

2.1. **Case 1.** We shall show the theorem when $b_p > 0$ and $b_q > 0$.

Lemma 2.5. *If* (1) $a_p \leq b_p$, $a_q \leq b_q$ *and* (2) $b_p > 0$, $b_q > 0$, *then there exists a* G*-map* $f\colon SV \to SW$.

Proof. By (1), there is an inclusion $i\colon SV^{>1} \to SW^{>1} \subset SW$. Using Waner's method [12], we show that this inclusion can be extended to a G-map f. Since G acts freely on $SV \setminus SV^{>1}$, SV is decomposed as a union of $SV^{>1}$ and free G-cells:

$$SV = SV^{>1} \cup G \times D^{n_1} \cup \cdots \cup G \times D^{n_r},$$

where $n_1 \leq \cdots \leq n_r$. Set $X_k = SV^{>1} \cup G \times D^{n_1} \cup \cdots \cup G \times D^{n_k}$, where $k \geq 1$. Suppose inductively that there is a G-map $f_{k-1}\colon X_{k-1} \to SW$, where $X_0 = SV^{>1}$ and $f_0 = i$. Since $X_k = X_{k-1} \cup G \times D^{n_k}$, restricting f_{k-1} to $1 \times \partial D^{n_k} = \partial D^{n_k}$, we have a map $g = f_{k-1}|_{\partial D^{n_k}}\colon \partial D^{n_k} \to SW$. Compose g with a G-map h of degree 0 and set $g' = h \circ g$. Then g' is null-homotopic and g' is extended to $g''\colon D^{n_k} \to SW$. Furthermore, g'' is equivariantly extended to a G-map $\tilde{g}\colon G \times D^{n_k} \to SW$. Thus we obtain a G-map $f_k = f_{k-1} \cup \tilde{g}\colon X_k \to SW$. □

2.2. **Case 2.** We shall show the theorem in the case of $b_p = 0$ or $b_q = 0$. We may suppose $b_q = 0$. Then by condition (1), we have $a_q = 0$ and $a_p \leq b_p$, If $a_1 \leq b_1$, then, there is an inclusion $i\colon SV \to SW$, which is G-equivariant.

Suppose that $a_1 > b_1$. By condition (2), we have $a_1 + a_p \leq b_1 + b_p$ and hence $a_1 - b_1 \leq b_p - a_p$. Note that there exists a G-map $g\colon SU_1 \to SU_p$; for example, g can be defined by $g(z) = z^p$. Hence there exists a G-map $\bar{g}\colon S((a_1-b_1)U_1) \to S((b_p-a_p)U_p)$ by Lemma 2.1. Joining $\bar{g}$ with the identity map $id\colon S(b_1U_1 \oplus a_pU_p) \to S(b_1U_1 \oplus a_pU_p)$, we obtain a G-map $f = \bar{g} * id\colon SV \to SW$. Thus the proof is complete.

3. Comparison to isovariant maps

Let G be a compact Lie group. A continuous G-map $f\colon X \to Y$ is called G-isovariant if f preserves the isotropy groups; i.e., $G_{f(x)} = G_x$ for all $x \in X$. It is

important to clarify the existence problem of isovariant maps and there are several researches about isovariant map as well as equivariant maps; for example, see [7], [8], [9], [10]. A necessary and sufficient condition for the existence of a C_{pq}-isovariant map between representations (or equivalently, representation spheres) is already known. In fact, the following result easily follows from results of [7].

Proposition 3.1. *Let $G = C_{pq}$. Let SV and SW be G-fixed point free (orthogonal) representation spheres. There exits a G-isovariant map $f\colon SV \to SW$ if and only if*

(1) $\dim V^H \leq \dim W^H$ *for* $H = C_p$ *and* C_q, *and*

(2) $\dim V - \dim V^H \leq \dim W - \dim W^H$ *for* $H = C_p$ *and* C_q.

Remark. By combining (1) and (2), it is deduced that $\dim V \leq \dim W$. This kind of result is called the isovariant Borsuk-Ulam theorem. See [10], [13] for more general results.

By comparing Proposition 3.1 and Theorem 1.6, we see that there are many pairs SV, SW of C_{pq}-fixed point free representation spheres such that there is a C_{pq}-map from SV to SW, but not a C_{pq}-isovariant map.

Example 3.2. Let $V = aU_1$ $(a \geq 1)$ and $W = U_p \oplus U_q$. Then there is a C_{pq}-map $f\colon SV \to SW$. However, if $a \geq 2$, then there is no C_{pq}-isovariant map from SV to SW.

This example provides another kind of Borsuk-Ulam type result; namely, if $a \geq 2$ and $f\colon SV \to SW$ is a C_{pq}-map, then it follows that $f^{-1}(SW^{>1}) \neq \emptyset$, where $SW^{>1}$ denotes the singular set of SW defined by $SW^{>1} = \{x \in SW \mid G_x \neq 1\}$. In this case, note that $SW^{>1} = SU_p \coprod SU_q$ (Hopf link). Furthermore, one can show the following.

Proposition 3.3. *Let $V = aU_1$ $(a \geq 2)$ and $W = U_p \oplus U_q$. If there is a C_{pq}-map $f : SV \to SW$, then $f^{-1}(SU_p) \neq \emptyset$ and $f^{-1}(SU_q) \neq \emptyset$.*

Proof. If $f^{-1}(SU_p) = \emptyset$, then we have an equivariant map $f\colon SV \to SW \setminus SU_p$. Since $SW \setminus SU_p$ is C_{pq}-homotopy equivalent to SU_q, there exists a C_{pq}-map $g\colon SV \to SU_q$. However, this contradicts Proposition 1.5 (2). Thus we see that $f^{-1}(SU_p) \neq \emptyset$. Similarly we see that $f^{-1}(SU_q) \neq \emptyset$. □

References

[1] T. Bartsch, *On the existence of Borsuk-Ulam theorems*, Topology **31** (1992), 533–543.

[2] T. tom Dieck, Transformation groups, *Transformation Groups*, Walter de Gruyter, Berlin, New York, 1987.
[3] E. Fadell and S. Husseini, *An ideal-valued cohomological index theory with applications to Borsuk-Ulam and Bourgin–Yang theorems*, Ergodic Theory Dynamical System **8** (1988), 73–85.
[4] T. Kobayashi, *The Borsuk-Ulam theorem for a $\mathbb{Z}_q$-map from a $\mathbb{Z}_q$-space to S^{2n+1}*, Proc. Amer. Math. Soc. 97 (1986), 714–716.
[5] W. Marzantowicz, *Borsuk-Ulam theorem for any compact Lie group*, J. Lond. Math. Soc., II. Ser. 49 (1994),195–208.
[6] W. Marzantowicz, D. de Mattos and E. L. dos Santos, *Bourgin-Yang version of the Borsuk-Ulam theorem for p-toral groups*, preprint.
[7] I. Nagasaki, *The converse of isovariant Borsuk-Ulam results for some abelian groups*, Osaka. J. Math. **43** (2006), 689-710.
[8] I. Nagasaki, *A note on the existence problem of isovariant maps between representation spaces*, Studia Humana et Naturalia 43 (2009), 33–42.
[9] I. Nagasaki, *Remarks on Borsuk-Ulam type results and the existence of isovariant maps*, Studia Humana et Naturalia 44 (2010), 91–100.
[10] I Nagasaki and F. Ushitaki, *New examples of the Borsuk-Ulam groups*, RIMS Kôkyuûoku Bessatsu **B39** (2013), 109–119.
[11] I. Nagasaki, T. Kawakami, Y. Hara and F. Ushitaki, *The Smith homology and Borsuk-Ulam type theorems*, Far East Journal of Mathematical Sciences (FJMS) **38** (2) (2010), 205-216.
[12] S. Waner, *A note on the existence of G-maps between spheres*, Proc. Amer. Math. Soc. **99** (1987), 179-181.
[13] A. G. Wasserman, *Isovariant maps and the Borsuk-Ulam theorem*, Topology Appli. **38** (1991), 155–161.

Bai et al. Molecular Brain 2013, 6:34
http://www.molecularbrain.com/content/6/1/34

Molecular Brain

RESEARCH Open Access

NMDA receptor subunits have different roles in NMDA-induced neurotoxicity in the retina

Ning Bai[1,4*], Tomomi Aida[1], Michiko Yanagisawa[1], Sayaka Katou[1], Kenji Sakimura[5], Masayoshi Mishina[6] and Kohichi Tanaka[1,2,3*]

Abstract

Background: Loss of retinal ganglion cells (RGCs) is a hallmark of various retinal diseases including glaucoma, retinal ischemia, and diabetic retinopathy. N-methyl-D-aspartate (NMDA)-type glutamate receptor (NMDAR)-mediated excitotoxicity is thought to be an important contributor to RGC death in these diseases. Native NMDARs are heterotetramers that consist of GluN1 and GluN2 subunits, and GluN2 subunits (GluN2A–D) are major determinants of the pharmacological and biophysical properties of NMDARs. All NMDAR subunits are expressed in RGCs in the retina. However, the relative contribution of the different GluN2 subunits to RGC death by excitotoxicity remains unclear.

Results: GluN2B- and GluN2D-deficiency protected RGCs from NMDA-induced excitotoxic retinal cell death. Pharmacological inhibition of the GluN2B subunit attenuated RGC loss in glutamate aspartate transporter deficient mice.

Conclusions: Our data suggest that GluN2B- and GluN2D-containing NMDARs play a critical role in NMDA-induced excitotoxic retinal cell death and RGC degeneration in glutamate aspartate transporter deficient mice. Inhibition of GluN2B and GluN2D activity is a potential therapeutic strategy for the treatment of several retinal diseases.

Keywords: NMDA receptor, GluN2B, GluN2D, Excitotoxicity, Retina, Glaucoma, Glutamate transporter

Background

Glutamate is the major excitatory neurotransmitter in the mammalian central nervous system. However, its accumulation in extracellular spaces kills neurons through excitotoxic mechanisms via activation of glutamate receptors [1]. Excitotoxic neuronal cell death is thought to be a final common pathway in various neurological diseases, ranging from acute ischemic stroke to chronic neurodegenerative diseases such as Alzheimer's disease and amyotrophic lateral sclerosis [2-5]. Glutamate excitotoxicity has also been proposed to be an important contributor to the death of retinal ganglion cells (RGCs) in glaucoma and ischemia-related conditions such as vessel occlusion and diabetic retinopathy [6-8], although some investigations have failed to confirm elevated glutamate concentration both in human patients with glaucoma [9] and in animal models of glaucoma [10,11]. The toxic effects of glutamate on RGCs are predominantly mediated by the overstimulation of N-methyl-D-aspartate (NMDA)-type glutamate receptors (NMDARs) due to their extreme permeability to calcium ions [12].

NMDARs are composed of various combinations of GluN1 and GluN2 (GluN2A–GluN2D) subunits and, in some cases, GluN3 (GluN3A and GluN3B) subunits. GluN2 subunits are major determinants of the functional properties of NMDARs, including characteristics such as agonist affinity, deactivation kinetics, single-channel conductance, Ca^{2+} permeability, and sensitivity to Mg^{2+} [13]. However, the relative contribution of different GluN2 subunits to RGC death by excitotoxicity remains unclear.

We previously reported that NMDAR-mediated excitotoxicity contributed to the degeneration of RGCs in glutamate aspartate transporter (GLAST) deficient (KO)

* Correspondence: bai.ning.aud@mri.tmd.ac.jp; tanaka.aud@mri.tmd.ac.jp
[1]Laboratory of Molecular Neuroscience, Medical Research Institute, Tokyo Medical and Dental University, 1-5-45 Yushima, Bunkyo-ku, Tokyo 113-8510, Japan
[2]The Center for Brain Integration Research, Tokyo Medical and Dental University, Tokyo, Japan
Full list of author information is available at the end of the article

mice, the first animal model of normal tension glaucoma [14]. Furthermore, we recently reported that GluN2D deficiency partially protected against the loss of RGCs in GLAST KO mice [15]. These results suggest that other GluN2 subunits, in addition to GluN2D, may contribute to excitotoxic retinal cell death. To address this hypothesis, we examined the roles of the four different GluN2 subtypes in NMDA-induced retinal cell death using mice lacking specific GluN2 subunits. We also evaluated the neuroprotective effect of 7-hydroxy-6-methoxy-2-methyl-1-(2-(4-(trifluoromethyl)phenyl)ethyl)-1,2,3,4-tetrahydroisoquinoline hydrochloride (HON0001) [16], an specific GluN2B antagonist, on RGC degeneration due to glutamate excitotoxicity in GLAST KO mice.

In the present study, we report that GluN2B and GluN2D deficiency protect against NMDA-induced excitotoxic retinal cell death, but GluN2A and GluN2C deficiency have no protective effects. We also show that pharmacological blockade of GluN2B subunit attenuates RGC loss in GLAST KO mice.

Results

NMDA receptor subunits present in mouse RGCs

To investigate the expression of NMDAR subunits in RGCs, we used a single-cell reverse transcriptase polymerase chain reaction (RT-PCR) method. After dissociation of the retina into single cells, RGCs can no longer be identified by their morphology. We therefore used dissociated retina from B6.Cg-TgN(Thy1-CFP)23Jrs/J transgenic mice (thy1-CFP mice), which express cyan fluorescent protein (CFP) in most RGCs [17]. We first confirmed that the CFP-containing cells in the thy1-CFP mouse retina were RGCs by immunostaining with Brn3, a neurochemical marker for RGCs [18]. CFP expression colocalized with Brn3 immunoreactivity in most somata in the ganglion cell layer (GCL) (Figure 1A-C). A single CFP-expressing cell was picked with a glass capillary from the dissociation mix and transferred to the reaction tube (Figure 1D, E), and was further identified as RGC by expression of Brn3 (Figure 1F). Typical results of single-cell RT-PCR on isolated RGCs are shown in Figure 1F. GluN1 and GluN2A–D could be amplified together with an internal control (β-actin) from a single RGC, as well as from whole retina. In our samples of 4 isolated RGCs, two cells express GluN1/GluN2A/GluN2B/GluN2C/GluN2D, whereas the other two cells express GluN1/GluN2A/GluN2B/GluN2D. These results indicate the presence of GluN1 and all GluN2 subunits (GluN2A–D) in the mouse RGCs.

Retinal structure in mice lacking GluN2 subunits

We used mice lacking any one of the four GluN2 subunits to determine the distinct roles of these GluN2 subunits in NMDA-induced RGC death. Mice lacking GluN2A,

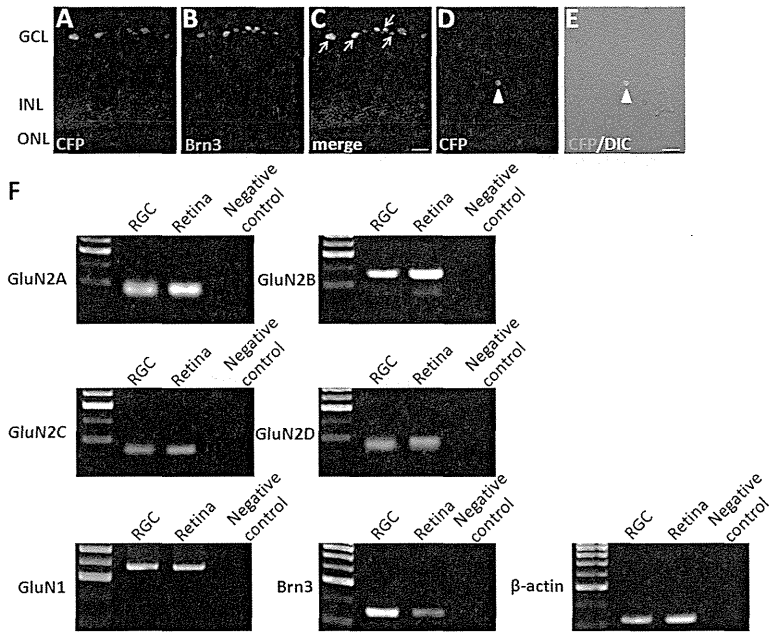

Figure 1 Expression of NMDA receptor subunits in mouse retinal ganglion cell. (A-C) Immunohistochemical analysis of Brn3 (**B** red) in Thy1-CFP mice. CFP fluorescence (**A** green) was overlaid with Brn3 **(C)**. Arrows in **(C)** indicate double-labeled cells. Scale bar, 20 μm. **(D-E)** After dissociation the fluorescent RGC was picked up from the cell suspension. CFP (green) and DIC pictures for the same isolated cell are superimposed **(E)**. Arrowhead indicates CFP-expressing RGC. Scale bar, 20 μm. **(F)** Single-cell RT-PCR analysis for GluN1, four GluN2 subunits, Brn3 and β-actin. Distilled water was used for PCR negative control. GCL, ganglion cell layer; INL, inner nuclear layer; ONL, outer nuclear layer; RGC, retinal ganglion cell.

GluN2C, and GluN2D are viable [19-21], whereas GluN2B-deficient mice die shortly after birth [22]. We therefore generated conditional GluN2B KO mice, in which GluN2B was ablated in retinal neurons containing RGCs. For this purpose, we crossed GluN2B$^{f/f}$ [23] mice with c-kit-Cre mice [24] (GluN2B$^{f/f}$/c-kit-Cre). In c-kit-Cre mice crossed with ROSA-tdTomato reporter mice [25] (ROSA-tdTomato/c-kit-Cre), tdTomato-expressing cells were localized in the GCL and inner nuclear layer (INL) and most calretinin immunoreactive cells (RGCs and amacrine cells) contained tdTomato, suggesting that Cre recombinase is expressed in RGCs and cells in the INL, including amacrine cells, in c-kit-Cre mice (Figure 2A). Immunohistochemical analysis revealed that GluN2B protein expression was eliminated in RGCs and cells in the INL in GluN2B$^{f/f}$/c-kit-Cre mice (Figure 2B). Western blot analysis showed that GluN2A, GluN2C, and GluN2D proteins were completely eliminated from mutant mice lacking GluN2A, GluN2C, and GluN2D, respectively (Figure 2C, E, F). In GluN2B$^{f/f}$/c-kit-Cre mice, GluN2B expression level in the retina was significantly lower than in control mice (Figure 2D).

We next investigated whether the absence of GluN2 subunits affects the anatomical organization of the retina by histological analyses. Hematoxylin and eosin staining revealed the retinae of GluN2A, GluN2B$^{f/f}$/c-kit-Cre, GluN2C, and GluN2D mutant mice to be normally organized, consisting of several different cell layers (Figure 3A). The thickness of the inner retinal layer (IRL) in all mutant strains was normal compared with wild-type (WT) mice (Figure 3B). As previous studies showed that ablation of GluN1 increased cell death in the developing somatosensory thalamus [26], we counted cell numbers in the GCL. The cell number in the GCL of GluN2B$^{f/f}$/c-kit-Cre mice was significantly lower than that of WT mice at 5 weeks, whereas cell number in the GCL of the other mutant strains was comparable to that of control mice at 5 weeks (Figure 3C). These results suggest that GluN2B subunit plays a survival role for RGCs during retinal development, but the other GluN2 subunits (GluN2A, GluN2C and GluN2D) are not involved in retinal development and survival in RGCs.

GluN2B and GluN2D deficiency prevents NMDA-induced-excitotoxic retinal cell death

To determine which GluN2 subtypes are involved in NMDA-induced RGC death in the retina, we examined the effect of intraocular injection of NMDA on retinal cell death in GluN2 KO and WT mice. First, to examine the acute injury of NMDA, TUNEL analysis was performed

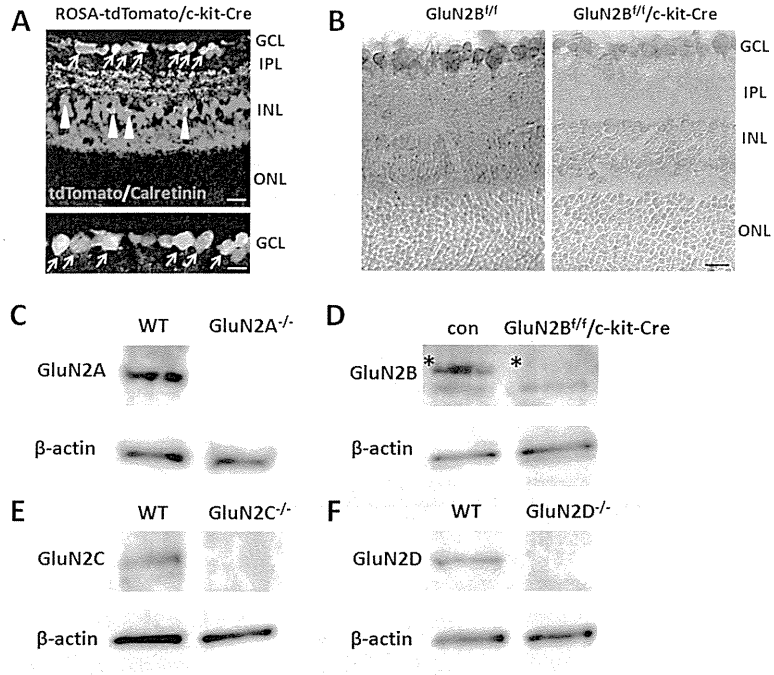

Figure 2 Ablation of GluN2 subunits in the retinas of mutant mice. (A) Immunostaining of calretinin (green) in ROSA-tdTomato/c-kit-Cre mice. Overlapping of tdTomato fluorescence (red) and calretinin indicated that Cre-mediated recombination occurs in RGCs (arrows) and amacrine cells (arrowheads). Enlarged image of the GCL in the upper panel was shown. Scale bar, 20 μm (upper) and 10 μm (lower). **(B)** Immunohistochemical analysis of GluN2B in GluN2B$^{f/f}$ and GluN2B conditional knockout mice (GluN2B$^{f/f}$/c-kit-Cre). Scale bar, 20 μm. **(C-F)** Western blot analysis of retinas from WT and GluN2 mutant mice with respective antibodies (GluN2A, GluN2B, GluN2C, GluN2D and β-actin). For GluN2B, control (con) represents GluN2B$^{f/f}$ mice. Asterisks indicate the GluN2B protein bands. Each lane was loaded with 30 μg of proteins. GCL, ganglion cell layer; IPL, inner plexiform layer; INL, inner nuclear layer; ONL, outer nuclear layer.

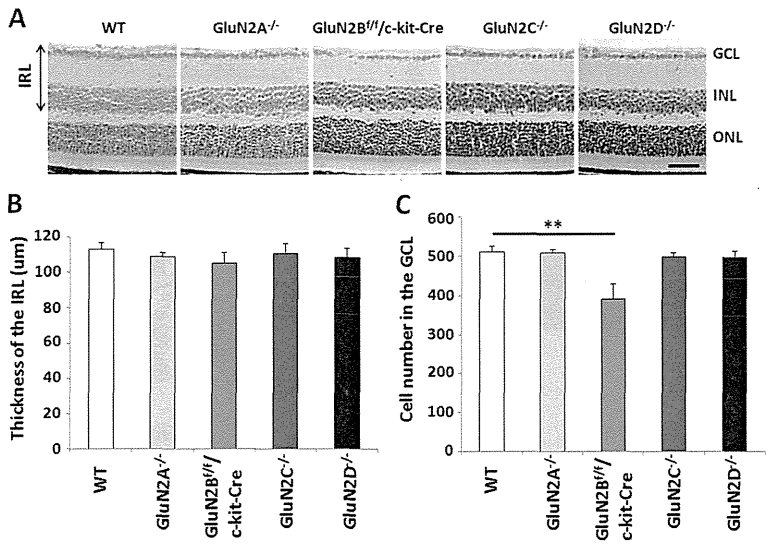

Figure 3 Effects of GluN2 subunits ablation on the morphology of the retina. (A) Hematoxylin and eosin staining (H&E) of retinal sections at P35 in WT and GluN2 mutant mice. Scale bar, 50 μm. **(B-C)** Quantification of thickness of the inner retinal layer **(B)** and the cell number in the GCL **(C)** in WT and GluN2 mutant mice. The data are presented as mean ± S.E.M. of 5 samples for each experiment. $^{**}P < 0.01$. GCL, ganglion cell layer; INL, inner nuclear layer; ONL, outer nuclear layer; IRL, inner retinal layer.

on the retinas of WT and GluN2 mutants at 1 day after NMDA treatment. A number of TUNEL-positive cells were observed in the GCL and INL in both WT and GluN2 mutant strains after NMDA injection (Figure 4A), but the percentage of TUNEL-positive cells in the GCL of GluN2B$^{f/f}$/c-kit-Cre and GluN2D$^{-/-}$ mice was significantly lower than that in WT mice (Figure 4B). Following NMDA injection, the number of RGCs and the thickness of IRL decreased from days 1 to 7, with no further decrease being observed from days 7 to 14 [27,28]. To examine the chronic injury of NMDA, morphological changes were measured 7 days after NMDA or phosphate-buffered saline (PBS) injection. Intraocular administration of NMDA induced cell death in the GCL in both WT and GluN2 mutant mice (Figure 4C), but the percentage of surviving cells in the GCL was significantly larger in GluN2B$^{f/f}$/c-kit-Cre and GluN2D$^{-/-}$ mice than in WT mice (Figure 4D). Additionally, the thickness of IRL was significantly larger in GluN2B$^{f/f}$/c-kit-Cre mice than in WT mice (Figure 4E). Taken together, these results suggest that GluN2B and GluN2D were involved in NMDA-induced RGC death.

A specific GluN2B antagonist, HON0001, prevents RGC death in GLAST-deficient mice

We have reported that the neuroprotective role of apolipoprotein E-containing lipoproteins in glaucomatous retinal degeneration in GLAST KO mice is mediated through promoting interaction between low density lipoprotein receptor-related protein 1 (LRP-1) and the GluN2B subunit [29]. Recently, we have also demonstrated that Dock3 overexpression prevented retinal cell death in GLAST KO mice by promoting GluN2B degradation [28]. To determine whether GluN2B is involved in RGC degeneration in GLAST-deficient mice, we evaluated the effect of a specific GluN2B antagonist, HON0001, on RGC degeneration in GLAST KO mice. As shown in Figure 5, the number of cells in GLAST KO mice subjected to HON0001 (10 mg/kg) treatment (281 ± 26) was significantly greater than that in GLAST KO mice not subjected to HON0001 treatment (203 ± 10). These results suggest that GluN2B is involved in RGC loss in GLAST KO mice.

Discussion

We previously reported that GluN2D deficiency prevented loss of RGCs in GLAST KO mice [15]. These results suggest that both GluN2B and GluN2D subunits play a critical role in RGC degeneration by glutamate excitotoxicity. Therefore, an GluN2B-selective antagonist in combination with an GluN2D-selective antagonist represents an effective strategy for the management of glaucoma and various forms of retinopathy. We recently showed that Dock3 overexpression prevented excitotoxic RGC death by suppressing the surface expression of GluN2D and enhancing NMDA-mediated GluN2B degradation [15,28]. Thus, the design of compounds capable of increasing the expression of Dock3 represents a novel strategy for the treatment of various forms of retinopathy. Previous studies also showed that calcium influx through NMDARs is modulated by LRP-1 [30,31]. These

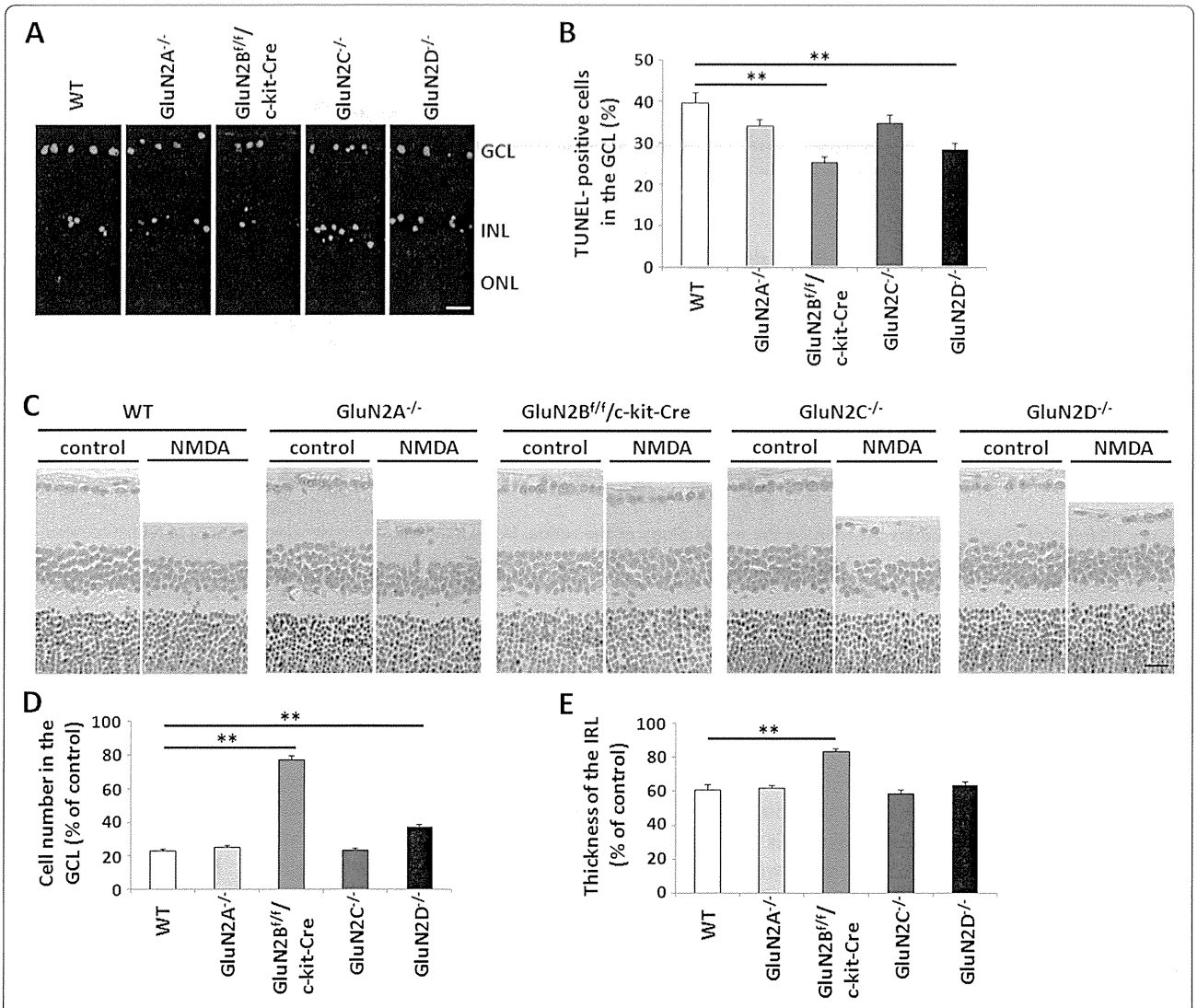

Figure 4 TUNEL staining and morphometric analysis following NMDA treatment. (A) Representative photos of TUNEL staining at 1 day after NMDA treatment from WT and GluN2 mutant mice. Scale bar, 20 μm. **(B)** Quantification of TUNEL-positive cells in the GCL. The data are presented as mean ± S.E.M. of 5 samples for each experiment. $^{**}P$ <0.01 **(C)** Representative photos of HE staining at 7 days after NMDA and PBS treatment from WT and GluN2 mutant mice. Scale bar, 20 μm. **(D-E)** Quantification of cell number in the GCL **(D)** and thickness of IRL **(E)**. The data are presented as mean ± S.E.M. of 5 samples for each experiment. $^{**}P$ <0.01. GCL, ganglion cell layer; INL, inner nuclear layer; ONL, outer nuclear layer; IRL, inner retinal layer.

findings may provide a novel therapeutic strategy for various forms of retinopathy that are mediated by E-containing lipoproteins through LRP-1.

The failure of GluN2C deficiency to protect RGCs from NMDA-induced excitotoxicity can be explained by the data showing that only a small number of RGCs expressed GluN2C [32]. However, almost RGCs express GluN2A [32]. The failure of GluN2A deficiency to protect RGCs from NMDA-induced excitotoxicity may be explained by the distinct functional properties conferred by GluN2 subunits on the receptors, and the different signaling pathway couplings [13,33]. This variety is due to the large and divergent cytoplasmic C-terminal domains of GluN2 subunits [34]. A previous report showed that C-terminal domains of GluN2B subunits were more lethal than GluN2A subunits, and different coupling to PSD-95/nNOS signaling cassette may contribute to differential susceptibility of GluN2 subunits to excitotoxic injury [33]. Another possible explanation is that the location of NMDARs at synaptic or extrasynaptic sites determines the neuroprotective or neurotoxic effects of glutamate. A high level of synaptic NMDAR activity promotes neuronal survival, whereas extrasynaptic NMDAR activity promotes cell death [35]. In the retina, GluN2B is

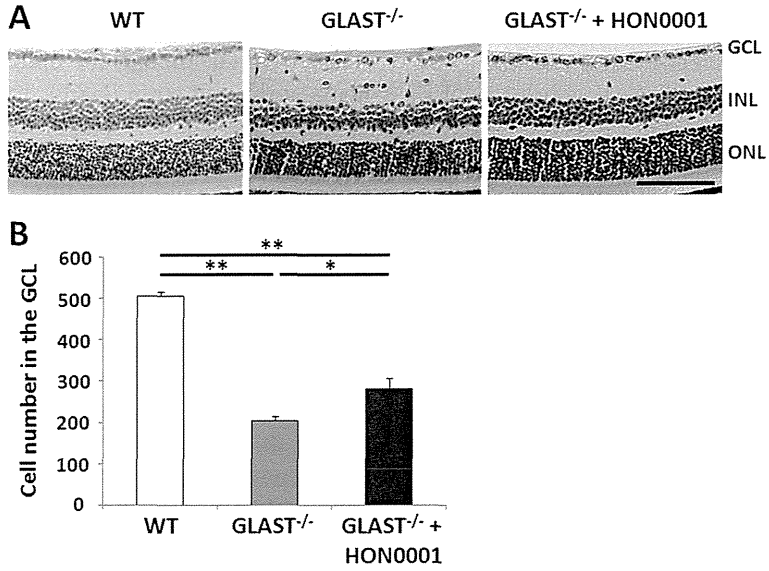

Figure 5 GluN2B antagonist HON0001 rescues RGCs death in GLAST-deficient mice. (A) Representative photos of wild-type (WT), saline- ($GLAST^{-/-}$) or HON0001- ($GLAST^{-/-}$ + HON0001) treated retinas. HON0001 (10 mg/kg) or saline were injected orally (p.o.) into $GLAST^{-/-}$ mice from P21 to P35. The animals were killed at P35 after HON0001/saline treatment. Scale bar, 100 μm. **(B)** Quantification of the cell number in the GCL. The data are presented as mean ± S.E.M. of 4 (WT and $GLAST^{-/-}$) and 6 ($GLAST^{-/-}$ + HON0001) samples for each experiment. *P <0.05, **P <0.01. GCL, ganglion cell layer; INL, inner nuclear layer; ONL, outer nuclear layer.

enriched at the perisynaptic site, whereas synaptic NMDARs primarily contain GluN2A [36].

The number of cells in the GCL of $GluN2B^{f/f}$/c-kit-Cre mice was significantly decreased at 5 weeks. This finding is consistent with a previous study showing that NMDAR hypofunction increased neuronal death in the developing brain [26,37]. GluN2B is a major GluN2 subunit in the immature retina [38]; therefore, ablation of GluN2B in the developing retina can cause excessive neuronal apoptosis, resulting in a reduction in the cell number in the GCL of $GluN2B^{f/f}$/c-kit-Cre mice. Thus, loss of GluN2B can increase RGC death in the immature retina, but protect RGCs from glutamate excitotoxicity in the adult.

Conclusions

We showed that GluN2B- and GluN2D-containing NMDARs played a critical role in NMDA-induced excitotoxic retinal cell death and RGC degeneration in GLAST KO mice. Inhibition of GluN2B and GluN2D activity is a potential therapeutic strategy for the treatment of several retinal diseases, including retinal ischemia, diabetic retinopathy, and glaucoma.

Methods

Animals

B6.Cg-TgN(Thy1-CFP)23Jrs/J transgenic mice (thy1-CFP mice) and c-kit-Cre transgenic mice have been described previously [17,24]. c-kit-Cre transgenic mice were bred with ROSA-tdTomato mice [25] to examine Cre activity. c-kit-Cre mice were bred with $GluN2B^{flox/flox}$ (*$GluN2B^{f/f}$*) mice [23] to generate GluN2B conditional knockout mice (*$GluN2B^{f/f}$/c-kit-Cre*). The homozygous GluN2A KO (*$GluN2A^{-/-}$*) [19], GluN2C KO mice (*$GluN2C^{-/-}$*) [20] and GluN2D KO mice (*$GluN2D^{-/-}$*) [21] were obtained by crossing heterozygous $GluN2A^{+/-}$, $GluN2C^{+/-}$ and $GluN2D^{+/-}$ mice, respectively. GLAST KO mice have been described previously [39,40]. In all experiments, age matched WT and $GluN2B^{f/f}$ littermate controls were used. All mice were of the C57BL/6 J genetic background, and all animal procedures were approved by the Animal Committee of Tokyo Medical and Dental University (0130166C).

Isolation of single ganglion cells from mouse retina and RT-PCR

5 week old Thy1-CFP mice were deeply anesthetized by diethyl ether and retinas were dissociated by using the Papain Dissociation System (Worthington Biochemical Corporation) at 37°C for 30 min. Single-CFP-expressing cell was aspirated by glass microcapillaries and placed into the PCR-tube containing 10 μl of resuspention buffer. Single-cell RT-PCR was performed using the SuperScript III CellsDirect cDNA Synthesis System (Invitrogen). Total RNA (5 μg) from whole retina were used to synthesize first-strand cDNA by using SuperScript III First-Strand Synthesis System (Invitrogen). The retina cDNA served as positive controls. The following primers were used for cDNA detection: GluN2A FWD: 5′ GTG TGC GAC CTC ATG TCC G 3′; REV: 5′ GCC TCT TGG TCC GTA TCA TCT C 3′; GluN2B FWD: 5′

CAG CAA AGC TCG TTC CCA AAA 3′; REV: 5′ GTC AGT CTC GTT CAT GGC TAC 3′; GluN2C FWD: ATC CCC GAC GGC TGA GA 3′; REV: 5′ TTC CTA GTC CAA GCA CAA AAC G 3′; GluN2D FWD: 5′ TGT GTG GGT GAT GAT GTT CGT 3′; REV: 5′ CCA CAG GAC TGA GGT ACT CAA AGA 3′; GluN1 FWD: 5′ GCC GAT TTA AGG TGA ACA GC 3′; REV: 5′ AAT TGT GCT TCT CCA TGT GC 3′; Brn3 FWD: 5′ GCA GTC TCC ACT TGG TGC TTA CTC 3′; REV: 5′ TTC CCC CTA CAA ACA AAC CTC C 3′; β-actin FWD: 5′ ATA TCG CTG CGC TGG TCG TC 3′; REV: 5′ TCA CTT ACC TGG TGC CTA GGG 3′. The thermal cycler conditions were 5 min at 94°C and then 40 cycles of 30 s at 94°C, 30 s at 60°C, and 30 s at 72°C, followed by 7 min at 72°C.

Western blot analysis

Retinas were quickly removed and homogenized in 100 μl of cold lysis buffer (50 mM Tris–HCl, 1% Nonidet P-40, 5 mM EDTA, 150 mM NaCl, 0.5% Na-deoxycholate, 1 mM $MgCl_2$, 1 mM DTT, 1 mM Na_3VO_4, 1 mM NaF, 1 mM phenylmethylsulfonyl fluoride (PMSF), and Complete Protease Inhibitor Cocktail [Roche]). Protein concentration was determined by BCA Protein Assay kit (Sigma-Aldrich). Thirty microgram of the protein was loaded per lane. Primary antibodies used were GluN2A (1:500, Covance), GluN2B (1:500) [41], GluN2C (1:100, Invitrogen), GluN2D (1:500) [42], β-actin (1:1000, Santa Cruz). They were then incubated with anti-rabbit, guinea pig or mouse IgG-HRP-conjugated secondary antibody (1:5000, Jackson ImmunoResearch). SuperSignal West Femto Maximum Sensitivity Substrate (Thermo Scientific) was used to visualize the immunoreactive proteins.

Immunohistochemistry

Sections were prepared as previously described [15]. Frozen retinal sections of 12 μm thickness were incubated using anti-Brn3 (1:50, Santa Cruz), anti-calretinin (1:500, Swant) and anti-GluN2B (1:100) antibodies. For Brn3 and calretinin detection, Cy-3-conjugated donkey anti-goat IgG (1:500, Jackson ImmunoResearch) and goat anti-rabbit IgG Alexa 488 (1:1000, Molecular Probes) were used as secondary antibodies. For GluN2B detection, peroxidase labelled polymer conjugated to goat anti-rabbit IgG (DAKO) was used as secondary antibody. Images were recorded with an LSM-510 META confocal laser microscope (Carl Zeiss).

Histology and morphometric analysis

Eyes from mice at postnatal day 35 (P35) were enucleated and fixed in Davidson's solution fixative [43], then embedded in paraffin wax. In some experiments, HON0001 (10 mg/kg, a gift from T. Honda at Hoshi University) [16] or saline was injected orally (p.o.) into GLAST KO mice daily from P21 to P35. These mice were sacrificed on P35 and processed for RGC count. Paraffin sections (7 μm thick) were cut though the optic nerve and stained with hematoxylin and eosin (H&E). The number of neurons in the GCL was counted as previously described [15]. The thickness of the IRL (from GCL to INL) was measured at a distance of 0.5 to 1.0 mm from optic disc.

Animal models of NMDA-induecd retinal neuronal death and morphometric analysis

Intravitreal injection of NMDA (Sigma) was conducted as previously described [15]. Briefly, a single 2-μl injection of 20 mM NMDA in 0.1 M PBS (pH 7.4) was administered intravitreally into the right eye of each mouse, the same volume of PBS was administered to the contralateral (left) eye as control. The animals were sacrificed at 1 day or 7 days after injection, and eyes were enucleated for morphometric and TUNEL analysis. Paraffin sections (5 μm thick) were cut though the optic nerve and stained with H&E. The extent of NMDA-induced retinal cell death after 7 days was quantified by counts of neurons in the GCL and the thickness of the IRL. The changes of the number of ganglion cells and thickness of IRL after NMDA injection were expressed as percentages of the control eyes.

TUNEL staining

At 1 day after the NMDA or PBS injection, TUNEL staining was performed with paraffin sections (5 μm thick) according to the manufacturer's instructions (Promega). Fluorescence detection was carried out using Alexa-fluor -568-conjugated streptavidin (Molecular Probes). TUNEL-positive cells in the GCL were counted and expressed as percentages of total DAPI stained cells in the GCL.

Statistics

Statistical analyses were conducted using Student's t-test for comparison between two samples, or one-way ANOVA followed by Bonferroni's test for multiple comparisons, using the SPSS 17.0 software package. Data are expressed as mean ± S.E.M. P values < 0.05 were considered statistically significant.

Abbreviations

GLAST: Glutamate aspartate transporter; INL: Inner nuclear layer; IPL: inner plexiform layer; IRL: Inner retina layer; LRP: lipoprotein receptor-related protein; NMDAR: N-methyl-D-aspartate receptor; PBS: Phosphate-buffered saline; PMSF: Phenylmethylsulfonyl fluoride; RGC: Retinal ganglion cell; RT-PCR: Reverse transcriptase polymerase chain reaction; WT: Wild-type.

Competing interests

The authors declare that they have no competing interests.

Authors' contributions

KT, NB, and TA conceived and designed the experiments. NB, SK and MY carried out experiments and analyzed the data. KS and MM contributed reagents and materials. KT and NB wrote the paper. All authors have read and approved the manuscript for publication.

Acknowledgements
We thank M. Watanabe and T. Honda for GluN2B and GluN2D antibody and for HON0001, respectively. We also thank Y. Hiraoka for technical support. This study was supported by "Understanding of molecular and environmental bases for brain health" executed under the Strategic Research Program for Brain Sciences from the Ministry of Education, Culture, Sports, Science and Technology, Japan (KT) and by the Ministry of health, Labor and Welfare of Japan (KT).

Author details
[1]Laboratory of Molecular Neuroscience, Medical Research Institute, Tokyo Medical and Dental University, 1-5-45 Yushima, Bunkyo-ku, Tokyo 113-8510, Japan. [2]The Center for Brain Integration Research, Tokyo Medical and Dental University, Tokyo, Japan. [3]JST, CREST, Saitama, Japan. [4]College of Basic Medicine, China Medical University, 92 Bei Er Road, Heping District, Shenyang 110001, China. [5]Department of Cellular Neurobiology, Brain Research Institute, Niigata University, Niigata 951-8585, Japan. [6]Brain Science Laboratory, The Research Organization of Science and Technology, Ritsumeikan University, Nojihigashi 1-1-1, Kusatsu, Shiga 525-8577, Japan.

Received: 11 July 2013 Accepted: 29 July 2013
Published: 31 July 2013

References

1. Choi DW: **Glutamate neurotoxicity and diseases of the nervous system.** *Neuron* 1988, **1**:623–634.
2. Choi DW, Rothman SM: **The role of glutamate neurotoxicity in hypoxic-ischemic neuronal death.** *Annu Rev Neurosci* 1990, **13**:171–182.
3. Chapman AG: **Glutamate and epilepsy.** *J Nutr* 2000, **130**(4S Suppl):1043S–1045S.
4. Meldrum B: **Amino acids as dietary excitotoxins: a contribution to understanding neurodegenerative disorders.** *Brain Res Brain Res Rev* 1993, **18**:293–314.
5. Kalia LV, Kalia SK, Salter MW: **NMDA receptors in clinical neurology: excitatory times ahead.** *Lancet Neurol* 2008, **7**:742–755.
6. Casson RJ: **Possible role of excitotoxicity in the pathogenesis of glaucoma.** *Clin Experiment Ophthalmol* 2006, **34**:54–63.
7. Kaur C, Foulds WS, Ling EA: **Hypoxia-ischemia and retinal ganglion cell damage.** *Clin Ophthalmol* 2008, **2**:879–889.
8. Hernández C, Simó R: **Neuroprotection in diabetic retinopathy.** *Curr Diab Rep* 2012, **12**:329–337.
9. Honkanen RA, Baruah S, Zimmerman MB, Khanna CL, Weaver YK, Narkiewicz J, Waziri R, Gehrs KM, Weingeist TA, Boldt HC, *et al*: **Vitreous amino acid concentrations in patients with glaucoma undergoing vitrectomy.** *Arch Ophthalmol* 2003, **121**:183–188.
10. Levkovitch-Verbin H, Martin KR, Quigley HA, Baumrind LA, Pease ME, Valenta D: **Measurement of amino acid levels in the vitreous humor of rats after chronic intraocular pressure elevation or optic nerve transection.** *J Glaucoma* 2002, **11**:396–405.
11. Carter-Dawson L, Crawford ML, Harwerth RS, Smith EL, Feldman R, Shen FF, Mitchell CK, Whitetree A: **Vitreal glutamate concentration in monkeys with experimental glaucoma.** *Invest Ophthalmol Vis Sci* 2002, **43**:2633–2637.
12. Ferreira IL, Duarte CB, Carvalho AP: **Ca2+ influx through glutamate receptor-associated channels in retina cells correlates with neuronal cell death.** *Eur J Pharmacol* 1996, **302**:153–162.
13. Cull-Candy S, Brickley S, Farrant M: **NMDA receptor subunits: diversity, development and disease.** *Curr Opin Neurobiol* 2001, **11**:327–335.
14. Harada T, Harada C, Nakamura K, Quah HM, Okumura A, Namekata K, Saeki T, Aihara M, Yoshida H, Mitani A, *et al*: **The potential role of glutamate transporters in the pathogenesis of normal tension glaucoma.** *J Clin Invest* 2007, **117**:1763–1770.
15. Bai N, Hayashi H, Aida T, Namekata K, Harada T, Mishina M, Tanaka K: **Dock3 interaction with a glutamate-receptor NR2D subunit protects neurons from excitotoxicity.** *Mol Brain* 2013, **6**:22.
16. Suetake-Koga S, Shimazaki T, Takamori K, Chaki S, Kanuma K, Sekiguchi Y, Suzuki T, Kikuchi T, Matsui Y, Honda T: **In vitro and antinociceptive profile of HON0001, an orally active NMDA receptor NR2B subunit antagonist.** *Pharmacol Biochem Behav* 2006, **84**:134–141.
17. Feng G, Mellor RH, Bernstein M, Keller-Peck C, Nguyen QT, Wallace M, Nerbonne JM, Lichtman JW, Sanes JR: **Imaging neuronal subsets in transgenic mice expressing multiple spectral variants of GFP.** *Neuron* 2000, **28**:41–51.
18. Xiang M, Zhou L, Peng YW, Eddy RL, Shows TB, Nathans J: **Brn-3b: a POU domain gene expressed in a subset of retinal ganglion cells.** *Neuron* 1993, **11**:689–701.
19. Sakimura K, Kutsuwada T, Ito I, Manabe T, Takayama C, Kushiya E, Yagi T, Aizawa S, Inoue Y, Sugiyama H: **Reduced hippocampal LTP and spatial learning in mice lacking NMDA receptor epsilon 1 subunit.** *Nature* 1995, **373**:151–155.
20. Kadotani H, Hirano T, Masugi M, Nakamura K, Nakao K, Katsuki M, Nakanishi S: **Motor discoordination results from combined gene disruption of the NMDA receptor NR2A and NR2C subunits, but not from single disruption of the NR2A or NR2C subunit.** *J Neurosci* 1996, **16**:7859–7867.
21. Ikeda K, Araki K, Takayama C, Inoue Y, Yagi T, Aizawa S, Mishina M: **Reduced spontaneous activity of mice defective in the epsilon 4 subunit of the NMDA receptor channel.** *Brain Res Mol Brain Res* 1995, **33**:61–71.
22. Kutsuwada T, Sakimura K, Manabe T, Takayama C, Katakura N, Kushiya E, Natsume R, Watanabe M, Inoue Y, Yagi T, *et al*: **Impairment of suckling response, trigeminal neuronal pattern formation, and hippocampal LTD in NMDA receptor epsilon 2 subunit mutant mice.** *Neuron* 1996, **16**:333–344.
23. Akashi K, Kakizaki T, Kamiya H, Fukaya M, Yamasaki M, Abe M, Natsume R, Watanabe M, Sakimura K: **NMDA receptor GluN2B (GluR epsilon 2/NR2B) subunit is crucial for channel function, postsynaptic macromolecular organization, and actin cytoskeleton at hippocampal CA3 synapses.** *J Neurosci* 2009, **29**:10869–10882.
24. Eriksson B, Bergqvist I, Eriksson M, Holmberg D: **Functional expression of Cre recombinase in sub-regions of mouse CNS and retina.** *FEBS Lett* 2000, **479**:106–110.
25. Madisen L, Zwingman TA, Sunkin SM, Oh SW, Zariwala HA, Gu H, Ng LL, Palmiter RD, Hawrylycz MJ, Jones AR, *et al*: **A robust and high-throughput Cre reporting and characterization system for the whole mouse brain.** *Nat Neurosci* 2010, **13**:133–140.
26. Adams SM, de Rivero Vaccari JC, Corriveau RA: **Pronounced cell death in the absence of NMDA receptors in the developing somatosensory thalamus.** *J Neurosci* 2004, **24**:9441–9450.
27. Endo K, Nakamachi T, Seki T, Kagami N, Wada Y, Nakamura K, Kishimoto K, Hori M, Tsuchikawa D, Shinntani N, *et al*: **Neuroprotective effect of PACAP against NMDA-induced retinal damage in the mouse.** *J Mol Neurosci* 2011, **43**:22–29.
28. Namekata K, Kimura A, Kawamura K, Guo X, Harada C, Tanaka K, Harada T: **Dock3 attenuates neural cell death due to NMDA neurotoxicity and oxidative stress in a mouse model of normal tension glaucoma.** *Cell Death Differ* 2013. doi:10.1038/cdd.2013.91.
29. Hayashi H, Eguchi Y, Fukuchi-Nakaishi Y, Takeya M, Nakagata N, Tanaka K, Vance JE, Tanihara H: **A potential neuroprotective role of apolipoprotein E-containing lipoproteins through low density lipoprotein receptor-related protein 1 in normal tension glaucoma.** *J Biol Chem* 2012, **287**:25395–25406.
30. Qiu Z, Strickland DK, Hyman BT, Rebeck GW: **alpha 2-Macroglobulin exposure reduces calcium responses to N-methyl-D-aspartate via low density lipoprotein receptor-related protein in cultured hippocampal neurons.** *J Biol Chem* 2002, **277**:14458–14466.
31. Martin AM, Kuhlmann C, Trossbach S, Jaeger S, Waldron E, Roebroek A, Luhmann HJ, Laatsch A, Weggen S, Lessmann V, *et al*: **The functional role of the second NPXY motif of the LRP1 beta-chain in tissue-type plasminogen activator-mediated activation of N-methyl-D-aspartate receptors.** *J Biol Chem* 2008, **283**:12004–12013.
32. Jakobs TC, Ben Y, Masland RH: **Expression of mRNA for glutamate receptor subunits distinguishes the major classes of retinal neurons, but is less specific for individual cell types.** *Mol Vis* 2007, **13**:933–948.
33. Martel MA, Ryan TJ, Bell KF, Fowler JH, McMahon A, Al-Mubarak B, Komiyama NH, Horsburgh K, Kind PC, Grant SG, *et al*: **The subtype of GluN2 C-terminal domain determines the response to excitotoxic insults.** *Neuron* 2012, **74**:543–556.
34. Ryan TJ, Emes RD, Grant SG, Komiyama NH: **Evolution of NMDA receptor cytoplasmic interaction domains: implications for organisation of synaptic signalling complexes.** *BMC Neurosci* 2008, **9**:6.
35. Hardingham GE, Bading H: **Synaptic versus extrasynaptic NMDA receptor signalling: implications for neurodegenerative disorders.** *Nat Rev Neurosci* 2010, **11**:682–696.
36. Zhang J, Diamond JS: **Subunit- and pathway-specific localization of NMDA receptors and scaffolding proteins at ganglion cell synapses in rat retina.** *J Neurosci* 2009, **29**:4274–4286.

37. Ikonomidou C, Bosch F, Miksa M, Bittigau P, Vöckler J, Dikranian K, Tenkova TI, Stefovska V, Turski L, Olney JW: **Blockade of NMDA receptors and apoptotic neurodegeneration in the developing brain.** *Science* 1999, **283**:70–74.
38. Watanabe M, Mishina M, Inoue Y: **Differential distributions of the NMDA receptor channel subunit mRNAs in the mouse retina.** *Brain Res* 1994, **634**:328–332.
39. Harada T, Harada C, Watanabe M, Inoue Y, Sakagawa T, Nakayama N, Sasaki S, Okuyama S, Watase K, Wada K, *et al*: **Functions of the two glutamate transporters GLAST and GLT-1 in the retina.** *Proc Natl Acad Sci USA* 1998, **95**:4663–4666.
40. Watase K, Hashimoto K, Kano M, Yamada K, Watanabe M, Inoue Y, Okuyama S, Sakagawa T, Ogawa S, Kawashima N, *et al*: **Motor discoordination and increased susceptibility to cerebellar injury in GLAST mutant mice.** *Eur J Neurosci* 1998, **10**:976–988.
41. Watanabe M, Fukaya M, Sakimura K, Manabe T, Mishina M, Inoue Y: **Selective scarcity of NMDA receptor channel subunits in the stratum lucidum (mossy fibre-recipient layer) of the mouse hippocampal CA3 subfield.** *Eur J Neurosci* 1998, **10**:478–487.
42. Wu Y, Kawakami R, Shinohara Y, Fukaya M, Sakimura K, Mishina M, Watanabe M, Ito I, Shigemoto R: **Target-cell-specific left-right asymmetry of NMDA receptor content in schaffer collateral synapses in epsilon1/NR2A knock-out mice.** *J Neurosci* 2005, **25**:9213–9226.
43. Chi ZL, Akahori M, Obazawa M, Minami M, Noda T, Nakaya N, Tomarev S, Kawase K, Yamamoto T, Noda S, *et al*: **Overexpression of optineurin E50K disrupts Rab8 interaction and leads to a progressive retinal degeneration in mice.** *Hum Mol Genet* 2010, **19**:2606–2615.

doi:10.1186/1756-6606-6-34
Cite this article as: Bai *et al.*: NMDA receptor subunits have different roles in NMDA-induced neurotoxicity in the retina. *Molecular Brain* 2013 **6**:34.

Cell Death and Differentiation (2013) 20, 1250–1256

www.nature.com/cdd

Dock3 attenuates neural cell death due to NMDA neurotoxicity and oxidative stress in a mouse model of normal tension glaucoma

K Namekata[1], A Kimura[1], K Kawamura[1], X Guo[1], C Harada[1], K Tanaka[2] and T Harada*[,1]

Dedicator of cytokinesis 3 (Dock3), a new member of the guanine nucleotide exchange factors for the small GTPase Rac1, promotes axon regeneration following optic nerve injury. In the present study, we found that Dock3 directly binds to the intracellular C-terminus domain of NR2B, an *N*-methyl-D-aspartate (NMDA) receptor subunit. In transgenic mice overexpressing Dock3 (Dock3 Tg), NR2B expression in the retina was significantly decreased and NMDA-induced retinal degeneration was ameliorated. In addition, overexpression of Dock3 protected retinal ganglion cells (RGCs) from oxidative stress. We previously reported that glutamate/aspartate transporter (GLAST) is a major glutamate transporter in the retina, and RGC degeneration due to glutamate neurotoxicity and oxidative stress is observed in GLAST-deficient (KO) mice. In GLAST KO mice, the NR2B phosphorylation rate in the retina was significantly higher compared with Dock3 Tg:GLAST KO mice. Consistently, glaucomatous retinal degeneration was significantly improved in GLAST KO:Dock3 Tg mice compared with GLAST KO mice. These results suggest that Dock3 overexpression prevents glaucomatous retinal degeneration by suppressing both NR2B-mediated glutamate neurotoxicity and oxidative stress, and identifies Dock3 signaling as a potential therapeutic target for both neuroprotection and axonal regeneration.
Cell Death and Differentiation (2013) **20,** 1250–1256; doi:10.1038/cdd.2013.91; published online 12 July 2013

Excitatory neurotransmission mediated by *N*-methyl-D-aspartate receptors (NMDARs), one of the ionotropic glutamate receptors, has fundamental roles in both physiological and pathological processes in the mammalian central nervous system (CNS). Overactivation of NMDA receptors is thought to be a key contributing factor in the pathophysiology of many CNS disorders, such as Alzheimer's disease[1,2] and Huntington disease.[3] Glutamate excitotoxicity is also implicated in the degeneration of the retinal ganglion cells (RGCs) and optic nerves observed under pathological conditions including glaucoma.[4,5] Consistently, we previously reported that loss of glutamate/aspartate transporter (GLAST) induces optic neuropathy without affecting intraocular pressure and exhibits many features similar to human normal tension glaucoma.[6]

NMDA receptors are tetramers that form functional receptor channels. Two NR1 subunits, which bind its co-agonist glycine, must combine with at least two NR2 (A–D) subunits, which bind glutamate.[7] In the retina, NMDARs on RGCs are activated by glutamate released from cone bipolar cells.[8] All four NR2 subunits are expressed in vertebrate retina, and both NR2A and NR2B are prevalent in the inner plexiform layer, where NMDARs are localized on RGC dendrites.[9–11] Among them, NR2B-containing receptors are shown to exhibit relatively high affinity both for glutamate and for the co-agonist glycine, prolonged channel opening and greater overall Ca^{2+} current per event.[12,13] It is well known that the intracellular C-terminus domain (CTD) of NR2B regulates the internalization and degradation of NR2B-containing receptors.[14–17] At postsynaptic sites, NR2B-CTD is phosphorylated at Tyr1472 by Fyn, thereby mediating complex formation of NMDA receptors with the postsynaptic density protein 95 (PSD95). This NMDAR-PSD95 interaction is required for excitotoxic downstream signaling.[17] Functionally, NR2B has been implicated in many forms of synaptic plasticity related to the physiology of striatal neurons and the pathogenesis of various neurological disorders.[18] Indeed, amyloid-β (Aβ) and tau protein promote Fyn-mediated NR2B stabilization at the plasma membrane, resulting in the enhancement of NMDAR-mediated neurodegeneration in the brain of a mouse model of Alzheimer's disease.[1,2,19]

Dedicator of cytokinesis 3 (Dock3), a new member of the guanine nucleotide exchange factors, is specifically expressed in neural cells and causes cellular morphological changes by activating the small GTPase Rac1.[20] We previously reported that Dock3 is primarily expressed in RGCs in the retina, and that Dock3 overexpression stimulates axonal regeneration after optic nerve injury *in vivo*.[21,22] Dock3 was initially identified as a binding protein to presenilin1,

[1]Visual Research Project, Tokyo Metropolitan Institute of Medical Science, Tokyo, Japan and [2]Laboratory of Molecular Neuroscience, School of Biomedical Science and Medical Research Institute, Tokyo Medical and Dental University, Tokyo, Japan
*Corresponding author: T Harada, Visual Research Project, Tokyo Metropolitan Institute of Medical Science, 2-1-6 Kamikitazawa, Setagaya-ku, Tokyo 156-8506, Japan. Tel: +81 3 6834 2338; Fax: +81 3 6834 2339; E-mail: harada-tk@igakuken.or.jp
Keywords: Dock3; glutamate; oxidative stress; neuroprotection; glaucoma
Abbreviations: Aβ, amyloid-beta; ASK1, apoptosis signal-regulating kinase 1; BDNF, brain-derived neurotrophic factor; CNS, central nervous system; CTD, intracellular C-terminus domain; Dock3, Dedicator of cytokinesis 3; GLAST, glutamate/aspartate transporter; GSK-3β, glycogen synthase kinase-3β; LDH, lactate dehydrogenase; NMDA, *N*-methyl-D-aspartate; PSD95, postsynaptic density protein 95; RGC, retinal ganglion cell
Received 01.4.13; revised 29.5.13; accepted 11.6.13; Edited by N Bazan; published online 12.7.13

a major causative gene of early-onset familial Alzheimer's disease.[23,24] Although the critical role of Dock3 in Alzheimer's disease is still unknown, it is reported that Dock3 is deposited and insolubilized in Alzheimer's disease brain.[23,25] In addition, a recent study reported that Rac1 activation mediated by Dock1 (Dock180), a homolog protein of Dock3, regulates endocytic membrane trafficking.[26] These observations suggest a possible interaction between Dock3 and NR2B, which may regulate NR2B expression in neural tissues. In addition, recent studies suggested a possibility that there is a causal relationship between Alzheimer's disease and glaucoma.[27,28] These observations prompted us to examine the interaction between Dock3 and NR2B in the retina, and the effects of Dock3 on GLAST-deficient (GLAST KO) mice that suffer from glaucoma-like RGC degeneration.[6]

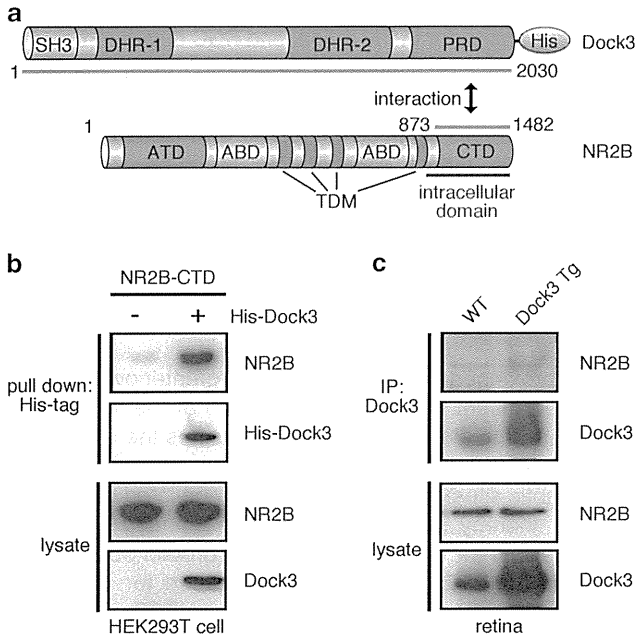

Figure 1 Dock3 interacts with the CTD of NR2B. (**a**) Schematic representation showing the His-tagged WT Dock3 and NR2B-CTD used in the pull-down assay. SH3, Src homology 3 domain; DHR-1, Dock homology region 1; DHR-2, dock homology region 2; PRD, proline-rich domain; ATD, amino-terminal domain; ABD, agonist binding domain; TDM, transmembrane domain; CTD, intracellular C-terminal domain. (**b**) Lysates from HEK293T cells transfected with His-tagged full-length Dock3 and NR2B-CTD were subjected to a His-tag pull-down assay. (**c**) Lysates from retinas of WT and Dock3 Tg mice were subjected to immunoprecipitation assay using an anti-Dock3 antibody

Results

Dock3 interacts with NR2B in the retina. We first examined whether Dock3 binds to NR2B in neural cells. For this experiment, we transfected His-tagged full-length Dock3 and CTD of NR2B (NR2B-CTD) (Figure 1a) to HEK293T cells and found that Dock3 binds to NR2B-CTD using His-tag pull-down assay (Figure 1b). We next examined whether Dock3 and NR2B are bound in neural tissues *in vivo*. The interaction between endogenous Dock3 and NR2B in wild-type (WT) mouse retina was confirmed by a co-immunoprecipitation assay (Figure 1c). We also found that the binding between Dock3 and NR2B was increased in Dock3 Tg mice, in which Dock3 is overexpressed in the retina (Figure 1c).[21]

We previously showed that Dock3 is abundantly expressed in retinal ganglion cells (RGCs) and stimulates axon outgrowth in adult mice.[21,22] Double-labeling immunohistochemistry showed that NR2B immunoreactivity was co-localized with Dock3 mainly in the ganglion cell layer (GCL) (Figure 2). These data support the binding of Dock3 and NR2B in RGCs of the adult retina *in vivo*.

Dock3 increases NMDA-mediated NR2B degradation in the retina. NMDA receptors undergo endocytosis and lysosomal sorting for receptor degradation.[14–18] As Dock3 and NR2B are bound in the retina, we investigated whether Dock3 affects NR2B degradation in the retina after NMDA stimulation. For this purpose, NR2B protein levels in the retinas from WT and Dock3 Tg mice were determined by immunoblot analysis at 3 and 24 h after the intraocular injection of phosphate-buffered saline (PBS; control) or NMDA. In the control retinas, NR2B expression levels in Dock3 Tg mice were not different compared with those in WT mice (Figure 3). NMDA injection had no effects on NR2B expression levels in the retina of WT mice, whereas NR2B expression levels were significantly decreased in Dock3 Tg mice (Figure 3). These results suggest that Dock3 enhances NR2B degradation due to glutamate neurotoxicity in the retina.

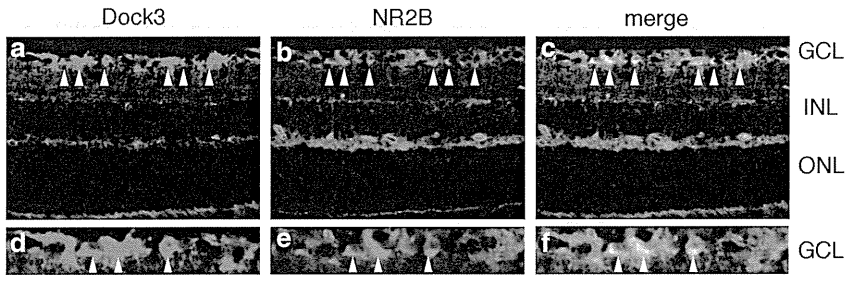

Figure 2 Expression of Dock3 and NR2B in the mouse retina. (**a–c**) Immunohistochemical analysis of mouse retina double-labeled (**c**) with antibodies against Dock3 (**a**) and NR2B (**b**). (**d–f**) Enlarged images of the GCL in (**a–c**), respectively. Arrow heads indicate double-labeled cells. GCL, ganglion cell layer; INL, inner nuclear layer; ONL, outer nuclear layer. Scale bar: 100 μm (**a–c**) and 50 μm (**d–f**)

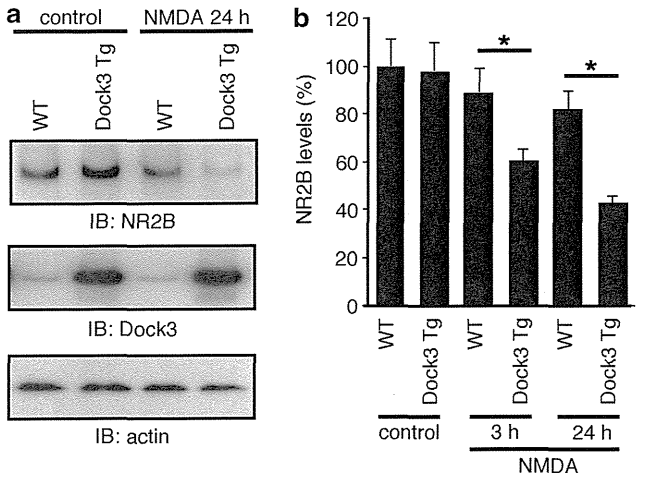

Figure 3 *Effect of Dock3 on NR2B expression levels in the retina.* (**a**) Immunoblot analysis of NR2B and Dock3 in the retinas of WT and Dock3 Tg mice 24 h after the injection of PBS (control) or NMDA. (**b**) Quantitative analysis of NR2B expression at 3 and 24 h after the injection of PBS (control) or NMDA. The data are presented as means ± S.E.M. of six samples for each experiment $^*P<0.05$

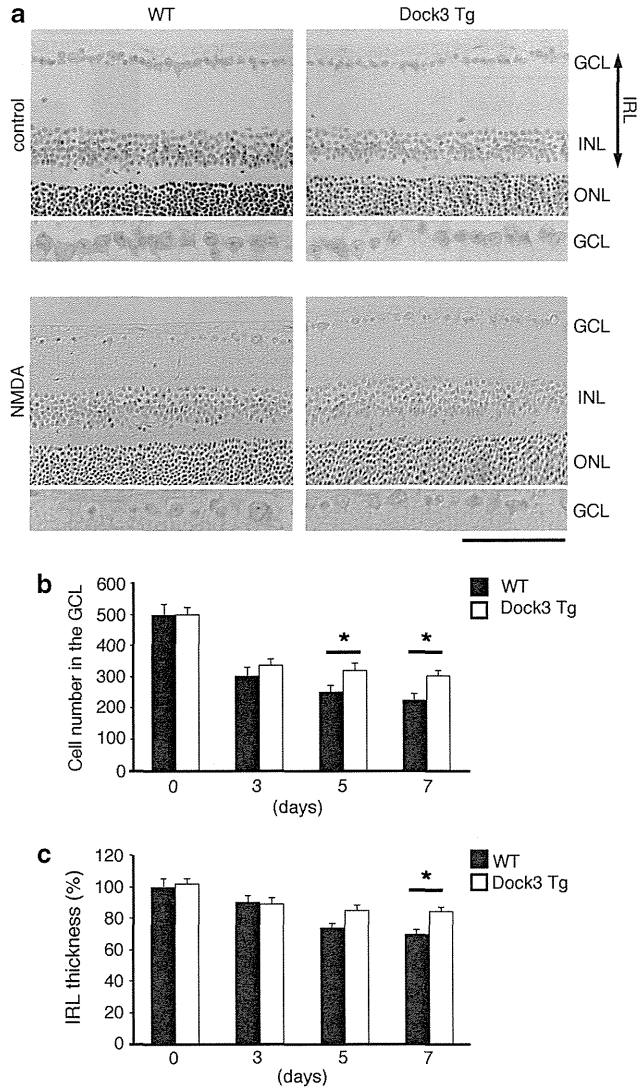

Figure 4 Dock3 protects retinal neurons from glutamate neurotoxicity. (**a**) H&E staining of retinal sections in WT and Dock3 Tg mice 7 days after intraocular treatment of PBS (control) or NMDA. Scale bar: 100 μm and 50 μm in the upper and lower panels, respectively. GCL, ganglion cell layer; INL, inner nuclear layer; ONL, outer nuclear layer. (**b** and **c**) Quantification of cell number in the GCL (**b**) and thickness of the inner retinal layer (**c**) at 0, 3, 5 and 7 days after NMDA treatment. The data are presented as means ± S.E.M. of six samples for each experiment $^*P<0.05$

Dock3 overexpression protects retinal neurons from glutamate neurotoxicity. Our present results suggest that overexpression of Dock3 in the retina may ameliorate glutamate neurotoxicity via NR2B degradation. To determine this possibility, we examined the effect of intraocular injection of NMDA on retinal cell death in WT and Dock3 Tg mice. The retinal structure of adult Dock3 Tg mice was normal, and the cell number in the GCL (497 ± 26; $n=6$) was comparable to WT mice (488 ± 31; $n=6$) (Figures 4a and b). In addition, the thickness of the inner retinal layer (IRL, between the internal limiting membrane and the interface of the outer plexiform layer and the outer nuclear layer) was similar in both strains (Figure 4c). Intraocular administration of NMDA induced cell death in the GCL in both WT and Dock3 Tg mice, but the number of surviving neurons in Dock3 Tg mice was significantly higher than that in WT mice at 5 and 7 days after NMDA injection (Figures 4a and b). Additionally, IRL thickness in Dock3 Tg mice was significantly increased at 7 days after NMDA injection compared with that in WT mice (Figure 4c). These results suggest that Dock3 overexpression prevents retinal cell death from glutamate neurotoxicity *in vivo*.

Dock3 overexpression protects RGCs from oxidative stress. Our previous study showed that oxidative stress, as well as glutamate neurotoxicity, induces RGC death.[29] To assess whether Dock3 also prevents oxidative stress-induced RGC death, cultured RGCs from WT mice were transfected with myc-tagged Dock3 plasmid by electroporation, and hydrogen peroxide (H_2O_2)-induced RGC death was assessed through the lactate dehydrogenase(LDH) leakage assays. Immunoblot analysis demonstrated that electroporation increased Dock3 expression levels in cultured RGCs (Figure 5a). The LDH leakage assay revealed that H_2O_2-induced cell death was significantly reduced in RGCs transfected with Dock3 plasmid compared with mock plasmid (Figures 5b and c). These results suggest that Dock3 overexpression protects RGCs from both glutamate neurotoxicity and oxidative stress.

Dock3 overexpression prevents glaucomatous retinal degeneration. We previously reported that glutamate neurotoxicity and oxidative stress are involved in RGC degeneration in GLAST KO mice, which is a mouse model of normal tension glaucoma.[6] In 3-month-old GLAST KO mice, the cell number in the GCL (325 ± 10; $n=6$) was significantly reduced compared with that in WT (479 ± 23; $n=6$) and Dock3 Tg (488 ± 21; $n=6$) mice (Figures 6a and b). Consistently, the thickness of the IRL was significantly reduced in GLAST KO mice compared with WT and Dock3 Tg mice (Figure 6c). As Dock3 may inhibit the two main